Arabian Journal of Chemical and Environmental Research

Vol. 13 Issue 3 (2026) 518–529

Adsorption of Cd(II) ion from aqueous solution using biochar derived millet straw

I. Abubakar

Department of Pure and Industrial Chemistry, Federal University Birnin Kebbi PMB 5711, Kebbi, Nigeria.

Email: kainuwailiyas@gmail.com.

Received 30 May 2026, Revised 19 July 2026, Accepted 21 July 2026

Cited as: *Abubakar Iliyasu (2026) Adsorption of Cd(II) ion from aqueous solution using biochar derived millet straw, Arab. J. Chem. Environ. Res. 13(3), 518-529*

Abstract

Adsorption ability of Millet straw derived biochar (BCM) pyrolysed at temperature (300 to 600 ºC) on Cd (II) in aqueous solution in an optimal operation parameter of pH (2-10), adsorbent dosage 0.3 to 1.1) g, concentration (30 to 250 mg/L), contact time (30 to 120) minutes, and temperature (318 to 333) K was investigated. The results showed that the biochar derived at higher pyrolysis temperatures (500 to 600 ºC) gave maximum uptake of Cd (II), this may be attributed to the abundance functional group and high surface area. However, the adsorption isotherm study indicated that the adsorption of Cd(II) onto BCM followed Langmuir isotherm with $R^2$0.99, indicating that the adsorption is monolayer adsorption. Furthermore, the adsorption kinetic study demonstrated that the adsorption of Cd by BCM is chemisorption, as Pseudo- Second Order gave the best fitting with the R^2 <0.99. The adsorption thermodynamic on the other hand, revealed that adsorption is spontaneous and endothermic. In conclusion, BCM can serve as a cost-effective and eco-friendly adsorbent for heavy metal adsorption.

Keywords: Biochar**;** Adsorption capacity; Adsorption kinetics; Adsorption isotherm; Adsorption thermodynamics

*Corresponding author.
E-mail address: kainuwailiyas@gmail.com

1. Introduction

World Health Organization characterised potentially toxic elements (PTEs) such as As, Pb, Cd Cr, and Hg as hazardous substances (Yang *et al.,* 2024). These elements enter ecosystems through various sources, including natural and human activities (such as industrial, transportation, soil mining etc) (Zhu *et al.,* 2020). These elements can accumulate in the living tissues, thereby causing various health complications, particularly in children (Yahya *et al.,* 2020; Basaran, 2025). Some of these complications include kidney disfunction, birth defects, immune system disfunction (Saha *et al.,* 2017; Sa *et al.,* 2022). However, considering the fact PTEs are non-biodegradable substance, it is has become imperative to

ISSN : 2458-6544

look into an effective route toward remediating the effects of these elements from the contaminated environment (Yahya *et al.,* 2020).

Pollutants such as heavy metals and dyes are removed from wastewater mainly through chemical precipitation, adsorption, membrane filtration, ion exchange, and electrochemical treatment. The choice of the most effective method depends on factors such as the specific metal involved, the initial concentration, and the overall treatment costs (Wang *et al.,* 2009; Errich *et al.,* 2021; Akartasse *et al.,* 2022; El Hammari *et al.,* 2022; Ayach *et al.,* 2024; S *et al.,* 2017; Sa *et al.,* 2022).

Biochar, a major product of pyrolysed biomass contains carbon as the major constituent element, as well as hydrogen, oxygen, ash, and trace amounts of nitrogen (Guagliano *et al.,* 2026). Owing to it specific properties, such as high pH and cation exchange capacity (CEC). The application of biochar as wastewater remediating agent continues to draw the attention of many researchers (Wang *et al.,* 2022). Meanwhile, studies have shown that biochar can effectively immobilize, decreases bioavailability and toxicity of PTEs from aqueous solution (Kumkum & Kumar, 2024). A research conducted by Tabana *et al* (2025) revealed that biochar derived from peanut hulls can effectively immobilized Cr(VI) ion from wastewater. Furthermore, study conducted by Zhu *et al* (2020) showed that a modified biochar (α-FeOOH@BC) could be an effective remedy material for Cd(II) and As(III) removal from aqueous environment.

2. Materials and methods

Our previous studies investigated the effect of pyrolysis temperature on physicochemical properties of millet straw derived biochar, where detailled experimental procedures were highlighted (Abubakar *et al.,* 2025). However, in a separate investigation on the effect of pyrolysis temperature on characteristics and adsorption of Pb(II) onto millet straw derived biochar from aqueous solution (Abubakar *et al.,* 2025), the findings demonstrated that increasing pyrolysis temperature significantly influenced the biochar's surface properties and lead adsorption capacity. However, the adsorption behaviour of Cd(II) by the same biochar has not yet been investigated.

2.1. Adsorption experiment

2.1.1. kinetic adsorption experiment

The adsorption kinetics experiment was conducted, 0.3 g each of the samples of biochar, was added to a 50 cm^3 centrifuge tube, followed by the addition of 40 cm^3 solutions of Cd(II). The initial pH of the solutions was adjusted to 6 using 0.1 $mol·L^{-1}$ hydrochloric acid and 0.1 $mol·L^{-1}$ sodium hydroxide. The tubes were placed in a mechanical shaker incubator at 37.5 ◦C and agitated at 120 rpm. Samples were withdrawn at predetermined time intervals of 5, 5, 10, 15, 20, 30, 60, 90, and 120 minutes, filtered through 0.45 µm, and analyzed for metal ion concentrations using atomic absorption spectrophotometry. Kinetic analysis of the adsorption process was performed using the pseudo-first-order, pseudo-second-order and Elovich kinetics models, and equations are given in (1), (2) and (3), respectively (Dada *et al.*, 2021):

$$q_t = q_e(1 - e^{-kt}) \quad (1)$$

$$qt = \frac{q_e^2 k_2 t}{1+q_e k_2 t} \quad (2)$$

$$q_t = \frac{1}{\beta} ln(1 + \alpha\beta t) \quad (3)$$

2.1.2. Isothermal Adsorption Experiment

Isothermal adsorption experiment was conducted using 0.3 g of BCM samples in a 50 cm^3 centrifuge tubes. 40 cm^3 of Cd metal ion solutions with varying concentrations of 30, 50, 100, 150 and 200 $mg·L^{-1}$ was added at an adjusted pH of 6 and 2 using 0.1 $mol·L^{-1}$ hydrochloric acid and 0.1 $mol·L^{-1}$ sodium hydroxide. The tubes were sealed and stirred with mechanical shaker at 37.5 ºC with agitation at 120 rpm for 90 minutes. After shaking, samples were centrifuged at 3000 rpm for 5 minutes and subsequently filtered through a 0.45 µm Whatman filter paper. The supernatants were collected in centrifuge tubes and analyzed for metal ion concentrations via atomic absorption spectrophotometry. The adsorption data of biochar samples for Cd(II) fitted using the Langmuir, Freundlich and Temkin isotherm models. Equations (4-6) as follow (Hu *et al.*, 2025):

$$qe = \frac{qmKLCe}{1+KLCe} \quad (4)$$

$$ln\, q\, e = ln\, K_F + \frac{1}{n} ln\, C\, e \quad (5)$$

$$q_e = B\, ln(K_T C_e) \quad (6)$$

2.1.3. Thermodynamic Adsorption Experiment

Thermodynamic experiments were performed at 45, 50, 55 and 60 °C. The temperature effect was established by adding 0.3 g of each biochar samples with 40 mL containing either 150 or 100mg L^{-1} Cd(II) in a temperature-controlled shaker at 45, 50, 55, and 60 ◦C at 120 rpm for 120 min initial solution pH 6.0. or 2.0 (Wang et al., 2025). Thermodynamic parameters such as free energy changes (ΔG, J mol^{-1}), enthalpy changes (ΔH, kJ mol^{-1}), and the entropy changes (ΔS KJ mol^{-1} K^{-1}) associated with the adsorption process was calculated using the relationship given in the following equations:

$$K_D = \frac{qe}{Ce} \quad (7)$$

$$\Delta G = -RT ln K_D \quad (8)$$

$$\ln K_D = \frac{\Delta H}{RT} - \frac{\Delta S}{R} \quad (9)$$

3. Results and discussion

3.1. Batch adsorption process

3.1.1 Effect of initial pH

In determining the biochar active site, the pH of the solution plays a crucial role (Zhao *et al*., 2020; Osman *et al.,* 2024). The pH in the range (2-10) was used to determine the effect it had on Cd^{2+} adsorption, and the result is presented in **Figure 1**. From the result, it can be observed that adsorption of Cd^{2+} onto BCM increased significantly ($p<0.05$), with the pH values increased from the said ranges, with the maximum adsorption at pH 6. However, beyond that the adsorption started to decline, indicating surface saturation. This proportional increase in Cd^{2+} adsorption with pH increase from 2-6 is attributed to the reduction in H^+ competition with cationic Cd metal as well as deprotonation of adsorbent's surfaces (Zhao et al., 2020). However, the critical pH at which adsorption initiated (the adsorption edge) varies systematically, as it occurred at a lower pH for low-temperature biochar's rich carboxylic groups (e.g., BCM400) and at a higher pH for high temperature, high-ash biochar (e.g., BCM600) where precipitation predominated (Chen et al., 2023).

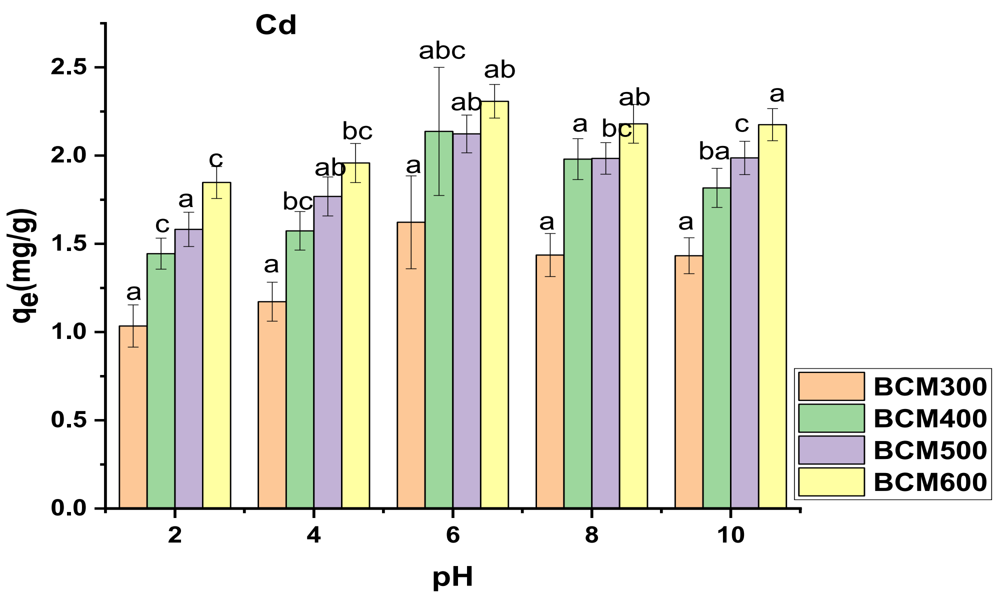

Figure 1: Effect of pH on the adsorption capacities of Cd(II) onto BCM

3.1.2. Adsorbent dose

The number of available sites and surface area depend largely on the biochar dose used, as this directly determines adsorbent–adsorbate interaction. **Figure 2** shows the result of the effect of BCM dose on the adsorption capacity of Cd(II) prepared at four different temperatures. The dosage effect of BCM (0.3 to 1.1 g/40 mL) standard solution on Cd (II) adsorption was investigated by varying the dose while keeping other variables constant. The results showed that increasing adsorbent dosage drastically decreases the adsorption capacity. This is due to the fact that high adsorbent dosage results in decreased active-site saturation (Mutanekelwa *et al.,* 2022). Hence, this causes a decline in the number of covered sites per unit mass of adsorbent, reducing the specific surface area, and resulting in a setback in the effective adsorption of the adsorbent (Reddy, 2019).

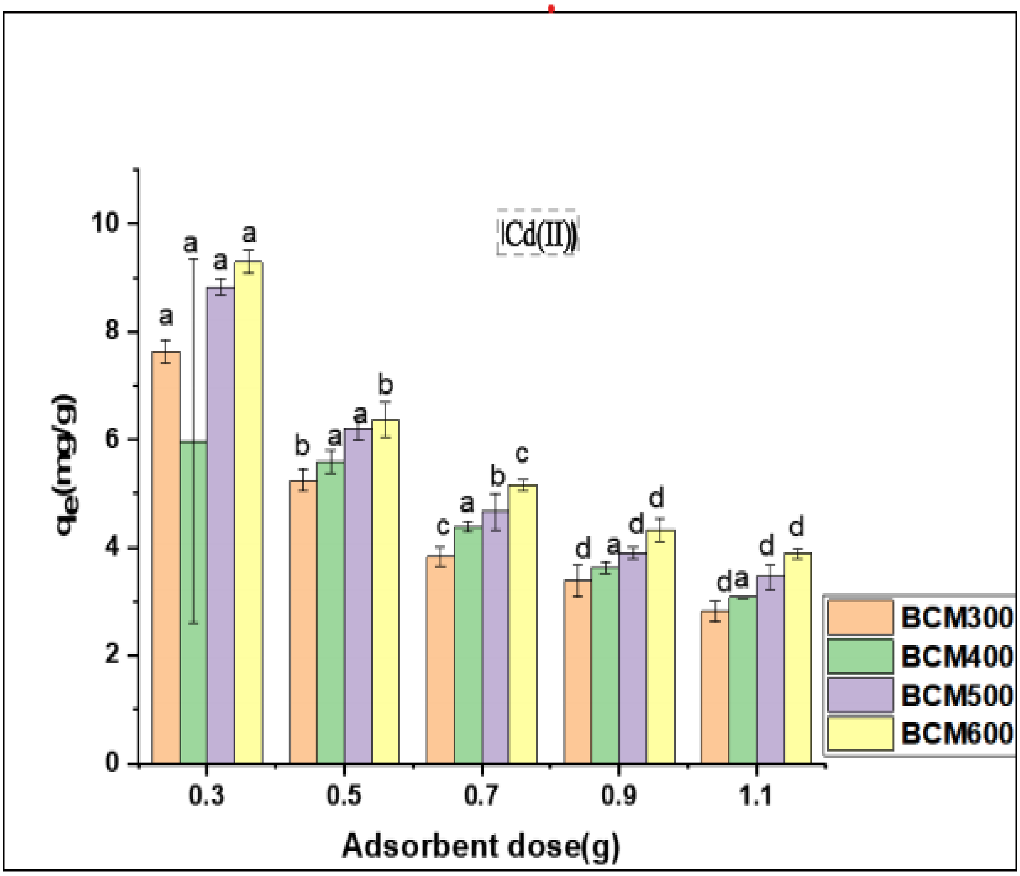

Figure 2: Effect of BCM dose on the adsorption capacity of Cd(II) prepared at four different temperatures

3.1.3. Adsorption isotherms

Table 1and Figure 3 show the results of Non-linear Langmuir, Freundlich and Temkin isothermal models to assess the effect of concentration on the adsorption of Cd^{2+} onto BCM. The results demonstrated that BCM produced at low pyrolysis temperatures (300–400°C) exhibited comparatively low maximum adsorption capacities (Qmax) due to incomplete carbonization, limited pore development, and low surface area (Gayathri *et al*., 2021). Despite the presence of oxygen-containing functional groups, the dominance of volatile matter and the absence of well-developed mineral phases constrained the number of effective adsorption sites (Di *et al*., 2025). However, at high pyrolysis temperatures (500–600°C), the biochar exhibits significantly higher maximum adsorption capacities (Qmax) for Cd compared to low-temperature biochar. This is due to strong influenced of the abundance of surface oxygen-containing functional groups, resulting in high Langmuir affinity parameter (R_L) values. This confirms that chemical affinity rather than surface area controlled Cd^{2+} adsorption onto BCM, particularly at lower pyrolysis temperatures (Yuan *et al.,* 2024). Therefore, the isothermal analysis reveals a fundamental design principle. BCM pyrolyzed at 500 °C emerged as a high-capacity adsorbent for Cd^{2+}, with adsorption behaviour that is well predicted by the Langmuir isotherm model Fig. 3**.** The excellent Langmuir fit suggests that Cd uptake on BCM500 occurs predominantly via monolayer adsorption on energetically uniform and structurally homogeneous sites (El Hammari *et al.*, 2023; Zhang *et al.*, 2023).

Table 1: Non-linear Langmuir, Freundlich and Temkin Isotherm adsorption parameters for Cd(II) onto BCM

Metal	Biochar		Langmuir			Freundlich			Temkin		
		$Q_{exp.}$	Qmax	K_L	R^2	K_F	n	R^2	b_T	K_T	R^2
	BCM300	8.12	8.25	0.0072	0.997	1.71	3.012	0.820	2.11	0.45	0.91
Cd(II)	BCM400	8.52	8.72	0.0085	0.997	1.74	2.958	0.833	2.23	0.43	0.92
	BCM500	8.92	9.17	0.0091	0.998	1.77	2.915	0.841	2.36	0.41	0.93
	BCM600	9.19	9.51	0.0099	0.999	1.89	2.976	0.840	2.41	0.44	0.93

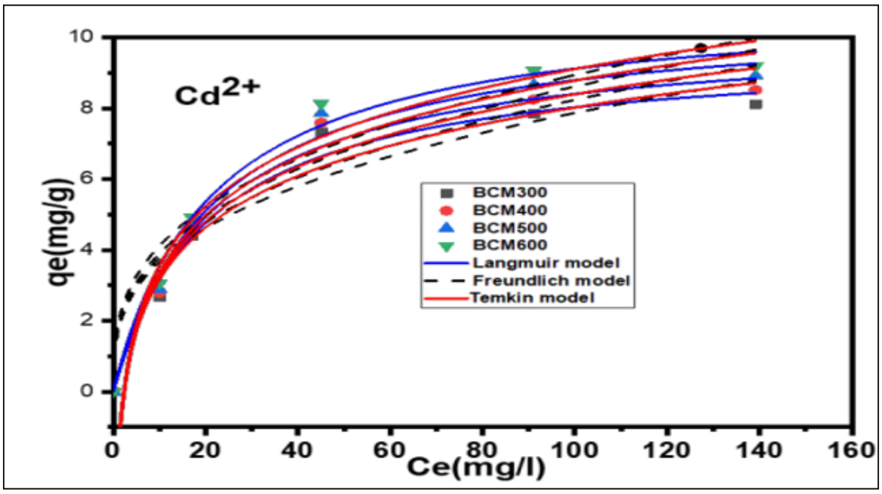

Figure 3: Non-linear Langmuir, Freundlich and Temkin isothermal models for adsorption of Cd^{2+} onto BCM.

3.1.4. Adsorption kinetics studies

The result of the effect of contact time on the adsorption capacity of Cd(II) by BCM at four different temperatures is presented in **Figure 4** and **Table 2**. From **Figure 4** it is observed that with the increase in time of contact, Cd (II) uptake by the biochar occurred in three stages. The first stage (initial stage), which is rapid occurred within the first 15 minutes of the process. This is due to abundance expose surface sites, which are quickly occupied at the initial stage and in a shorter possible time. The steeper slope, indicating faster initial, due to the abundance of available sites onto the biochar surface (Cuixia *et al*., 2020). However, the second stage (diffusion stage), this stage is gradually slow with increased in contact time, due to decreased in concentration and potential pores diffusion limitation. The final stage (equilibrium stage), which was established after 90 minutes for the biochar, which indicates that the saturation reached, and that the rate of adsorption equals rate of desorption (Wang *et al*., 2025). However, the kinetic models showed that that adsorption of Cd(II) onto BCM and produced at low pyrolysis temperature (300-400 ºC) are commonly best described by the pseudo-second-order (PSO) kinetic model **(Table 2),** indicating that the rate-limiting step is dominated by chemisorption processes rather than simple physical diffusion (Long *et al*., 2023). Similarly, the strong agreement in the metal uptake at lower pyrolysis temperatures between experimental and predicted adsorption capacities of the PSO models replicates the importance of surface chemical interactions in metal uptake at lower pyrolysis temperatures (Teğin *et al*., 2025)**.** This is due to the fact event at under developed pores at low pyrolysis temperature, the relatively abundance of oxygen-containing functional groups, including hydroxyl (–OH), carboxyl (–COOH), carbonyl (C=O), and phenolic groups, at low pyrolysis temperature biochar may show fast uptake due to readily available surface sites suitable for PSO model (Wang *et al*., 2025).

Table 2: Nonlinear PFO,PSO and Elovich Parameters for Cd (II) adsorption by BCM

Metal	Biochar	Nonlinear Pseudo-First Order				Nonlinear Pseudo-Second-Order			Elovich		
		$q_{e\ exp}$	$q_{e\ cal.}$	K_1	R^2	$q_{e\ cal}$	K_2	R^2	a	b	R^2
Cd (II)	BCM300	7.69	7.37	0.304	0.852	7.71	0.0878	0.977	59532.14	2.115	0.81
	BCM400	8.10	7.78	0.306	0.993	8.13	0.0843	0.999	75668.33	2.029	0.99
	BCM500	8.52	8.18	0.309	0.995	8.54	0.0827	0.998	139473	2.004	0.99
	BCM600	8.89	8.58	0.333	0.995	8.92	0.0905	0.998	810889.75	2.119	0.99

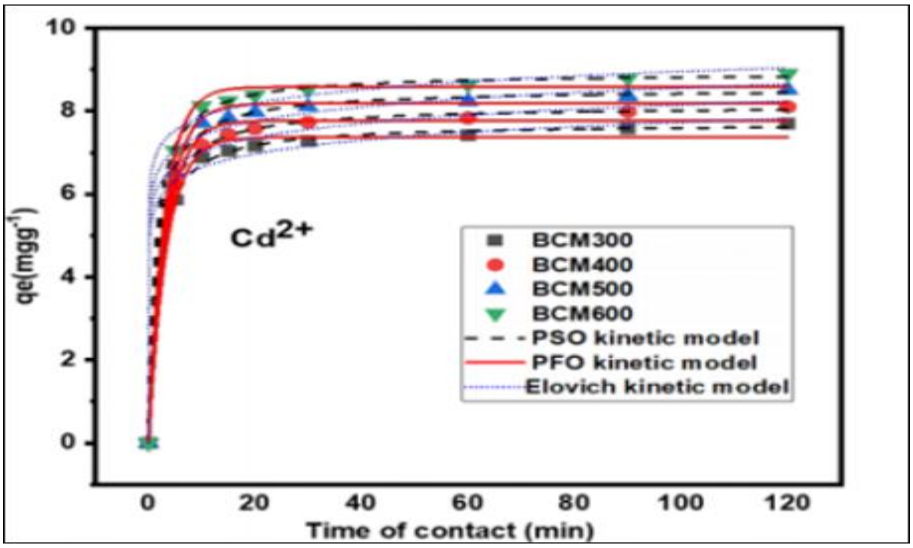

Figure 4: Non-linear PFO, PSO, and Elovich models for the adsorption of Cd (II) at different temperatures

3.1.5. Adsorption thermodynamic

In the present study the effect of solution temperature was investigated at intervals of 318 K, 323 K, 328K, and 333 K. The result is presented in **Table 3.** The results showed a positive enthalpy change (ΔH° > 0), this indicates that the adsorption process is endothermic, meaning that adsorption is favoured at higher temperatures (Ata *et al.*, 2023).

Table 3: Thermodynamic Parameters for Adsorption of Cd(II) onto BCM at four different temperatures

Biochar	Temperature (K)	ΔG ($Jmol^{-1}$)	ΔH(Jmo^{-1})	ΔS ($KJmol^{-1}$)	R^2
BCM300	318	-71.55	12743	40.27	0.99
	323	-273.86			
	328	-435.14			
	333	-690.14			
BCM400	318	-170.04	13404	42.75	0.89
	323	-477.69			
	328	-523.55			
	333	-867.87			
BCM500	318	-6513.41	12397	59.48	0.95
	323	-6786.31			
	328	-7176.94			
	333	-7372.95			
BCM600	318	-595.59	16853	54.81	0.97
	323	-848.45			
	328	-1058.73			
	333	-1441.58			

In biochar systems, this behaviour suggests that energy is required to overcome barriers such as dehydration of metal ions (Cd^{2+}), specific chemical interaction, diffusion into internal pores, or restructuring of surface sites before effective adsorption can occur (Li, 2020). The positive entropy change (ΔS° > 0) also observed implies an increase in randomness at the solid–solution interface during adsorption. Although adsorption is often intuitively associated with decreased disorder, in aqueous systems this apparent contradiction is resolved by considering the desolation of hydrated metal ions. When metal ions bind to biochar surfaces, structured water molecules surrounding the ions are released into the bulk solution, and increase freedom of the displaced ions (e.g., Ca^{2+}, H^{+}) released via ion exchange as well as the large positive ΔS, suggests a greater increase in randomness, after associated with process involving ion exchange or dehydration, resulting in a net increase in entropy (Nguyen *et al.*, 2025). Additionally, the higher correlation coefficient R^2 values of all the adsorbents are in the range R^2= 0.89-0.99 **Table 3**, suggesting that Van't Hoff's thermodynamic model provides a good fit to the experimental data, and this confirms the reliability of the thermodynamic parameters obtained (Sahmoune, 2019).

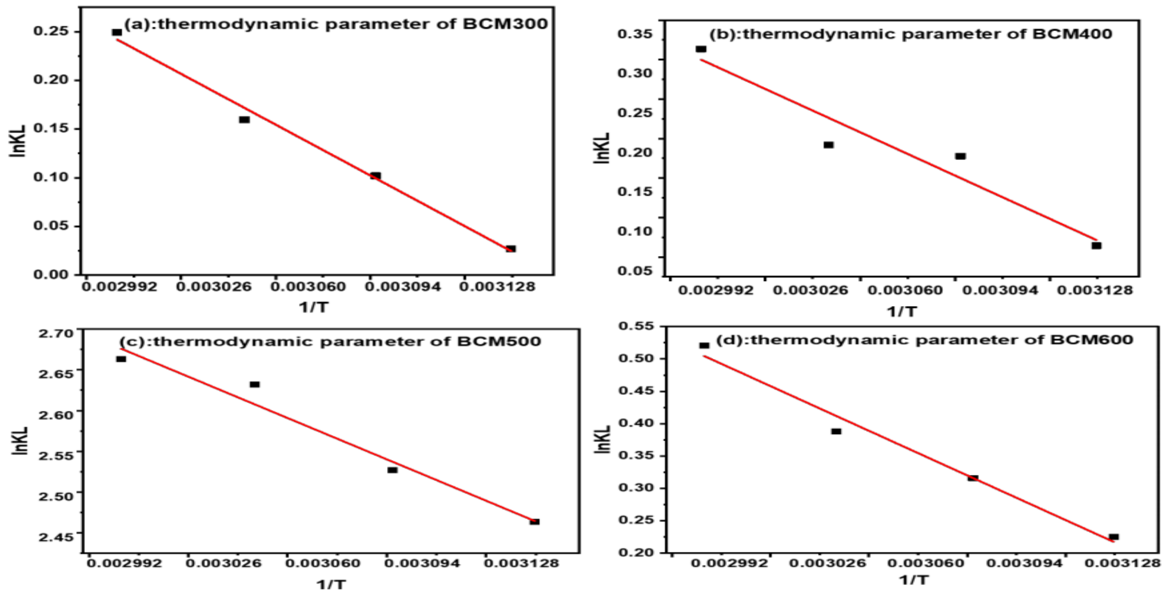

Figure 5: Van't Hoff's plot for the adsorption of Cd(II) onto BCM prepared at four different temperatures.

Conclusion

Biochar was generated using millet straw at 300-600 ºC pyrolysis temperatures to investigate its adsorption behaviour on Cd from aqueous solutions. Pyrolysis temperature strong effect on the structural and chemical properties of the biochar. Higher (500–600 °C) generated biochar exhibits aromatic behaviour, higher surface area, and higher ash content, and all these have positive impact on the biochar sorption capacity of metals via precipitation and electrostatic interactions. The adsorption isotherm study showed that the adsorption of Cd by BCM, can best be described by Langmuir isotherm model, indicating monolayer adsorption on relatively homogeneous sites. Moreover, adsorption kinetic studies revealed that the adsorption of Cd onto BCM followed the pseudo-second-order kinetic model**,** indicating that the rate-limiting step is governed by chemisorption involving electron sharing or exchange. Thermodynamic analyses showed negative Gibbs free energy (ΔG) values for all systems, confirming that the adsorption processes were spontaneous**.** The positive enthalpy (ΔH) values indicated that adsorption was endothermic, while positive entropy (ΔS) values suggested increased randomness at the solid–solution interface, likely due to the displacement of water molecules during metal binding.

Conflict of Interest: The author declares that no any conflict of interest in the conduct of the research.

References

Abubakar, I., Saeed, M. D., & Ayuba, A. M. (2025). Effect of pyrolysis temperature on characteristics and adsorption of Pb (II) onto millet straw derived biochar from aqueous solution. *Arabian*

Journal of Chemical and Environmental Research, *12*(2), 80–99.

Abubakar I., Saeed M.D., Muhammad A.A. (2025). Effect of pyrolysis temperature on physicochemical properties of Millet Straw derived biochar. *Green and Applied Chemistry*, *22*, 39–55.

Akartasse N., Azzaoui K., Mejdoubi E., Hammouti B., Elansari L.L., Abou-salama M., Aaddouz M., Sabbahi R., Rhazi L. and Siaj M. (2022), Environmental-Friendly Adsorbent Composite Based on Hydroxyapatite/Hydroxypropyl Methyl-Cellulose for Removal of Cationic Dyes from an Aqueous Solution, *Polymers,* 14(11), 2147; https://doi.org/10.3390/polym14112147

Ata, S., Tabassum, A., Shaheed, I., Mohsin, I., Alwadai, N., Huwayz, M. Al, Iqbal, M., & Nazir, A. (2023). Adsorption Thermodynamics, Modeling, and Kinetics Studies for the Removal of Lead Ions Using ZnO Nanorods. *Adsortion Science and Technology*, *2023*, 1–10.

Ayach J., El Malti W., Duma L., Lalevée J., Al Ajami M., Hamad H., Hijazi A. (2024). Comparing Conventional and Advanced Approaches for Heavy Metal Removal in Wastewater Treatment: An In-Depth Review Emphasizing Filter-Based Strategies. *Polymers.* 16(14), 1959. https://doi.org/10.3390/polym16141959

Basaran B. (2025). Occurrence of Potentially Toxic Metals Detected in Milk and Dairy Products in Türkiye: An Assessment in Terms of Human Exposure and Health Risks. *Foods.* 14(15), 2561. https://doi.org/10.3390/foods14152561

Cuixia Y., Yingming X., Lin W., Xuefeng L., Yuebing S. (2020). Effect of different pyrolysis temperatures on physico-chemical characteristics and lead(II) removal of biochar derived from chicken manure. *Royal Society of Chemistry*, *10*, 3667–3674. https://doi.org/10.1039/c9ra08199b

Dada, A. O., Adekola, F. A., Odebunmi, E. O., & Ogunlaja, A. S. (2021). Two – three parameters isotherm modeling , kinetics with statistical validity , desorption and thermodynamic studies of adsorption of Cu (II) ions onto zerovalent iron nanoparticles. *Scientific Reports*, 1–15. https://doi.org/10.1038/s41598-021-95090-8

El Hammari L., Latifi S., Saoiabi S., Saoiabi A., Azzaoui K., Hammouti B., *et al*. (2022), Toxic heavy metals removal from river water using a porous phospho-calcic hydroxyapatite, *Mor. J. Chem.* 10(1), 62-72, https://doi.org/10.48317/IMIST.PRSM/morjchem-v10i1.31752

El Hammari L., Hamed R., Khalil A., Jodeh S., Latifi S., Saoiabi S., Boukra O., Krime A., Boukra A., Saoiabi A., Hammouti B., Khan M. M., Sabbahi R., Hanbali G. and Berisha A., Taleb M., Dagdag O. (2023). Optimization of the Adsorption of Lead (II) by Hydroxyapatite using a Factorial Design: DFT and Molecular Dynamic, *Frontiers in Environmental Science,* 11, 1112019, doi: 10.3389/fenvs.2023.1112019

Errich A., Azzaoui K., Mejdoubi E., Hammouti B., Abidi N., Akartasse N., Benidire L., EL Hajjaji S., Sabbahi R., Lamhamdi A. (2021), Toxic heavy metals removal using a hydroxyapatite and hydroxyethyl cellulose modified with a new Gum Arabic, *Indonesian Journal of Science & Technology*, 6(1), 41-64

Guagliano, M., Reggi, S., Anno, M. D., Mostoni, S., Ottani, F., Puglia, M., Dotelli, G., Scotti, R., Pedrazzi, S., Rossi, L., Cristiani, C., & Finocchio, E. (2026). Smart waste - derived materials for feed application : chestnut shells and vine pruning biochar. *Biochar*, *8*(39), 1–22.

Hu, J., Yang, S., Ma, P., & Deng, Z. (2025). Adsorption of Cu (II), Pb (II), Cd (II), and Cr (III) from aqueous solutions using modified coffee grounds biochar. *Desalination and Water Treatment*, *323*(June), 101262. https://doi.org/10.1016/j.dwt.2025.101262

Kumkum, P., & Kumar, S. (2024). A Review on Biochar as an Adsorbent for Pb (II) Removal from Water. *Biomass*, (Ii), 243–272.

Li, Y. (2020). Adsorption behaviors on trace Pb 2 þ from water of biochar adsorbents from konjac starch. *Adsortion Science and Technology*, *38*(9–10), 344–356. https://doi.org/10.1177/0263617420948699

Long, X., Zhang, R., Rong, R., Wu, P., Chen, S., Ao, J., An, L., & Fu, Y. (2023). Adsorption Characteristics of Heavy Metals Pb^{2+} and Zn^{2+} by Magnetic Biochar Obtained from Modified AMD Sludge. *Toxics*.

Nguyen, H. H. T., Choi, Y. H., Kim, E. B., Jeong, Y. H., Lee, J. W., Park, K. H., Woo, Y. J., Ameen, S., & Kwak, D. H. (2025). Investigation of Pb(II) adsorption by amine group enriched chitosan encapsulated iron oxides doped biochar for soil remediation. *Carbon Trends*, *19*(January), 100465. https://doi.org/10.1016/j.cartre.2025.100465

Sa, M., Ahmed, Z., Munir, S., Reza, A., Rabia, T., Ara, B., & Idris, A. M. (2022). Assessment of heavy metal contamination in sediment at the newly established tannery industrial Estate in Bangladesh : A case study. *Environmental Chemistry and Ecotoxicology*, *4*(September 2021), 1–12. https://doi.org/10.1016/j.enceco.2021.10.001

Saha N., M.S. Rahman, M.B. Ahmed, J.L. Zhou (2017). Industrial metal pollution in water and probabilistic assessment of human health risk, *J. Environ. Manag.,* 185, 70-78 https://doi.org/10.1016/j.jenvman.2016.10.023

Sahmoune, M. N. (2019). Evaluation of thermodynamic parameters for adsorption of heavy metals by green adsorbents. *Environmental Chemistry Letters*, (October 2018). https://doi.org/10.1007/s10311-018-00819-z

Tabana, L., Kupa, A., & Tichapondwa, S. (2025). Adsorption of hexavalent chromium from wastewater using magnetic biochar derived from peanut hulls. *Physics and Chemistry of the Earth*, *137*(March 2024), 103815. https://doi.org/10.1016/j.pce.2024.103815

Wang, Y., Qiu, M., Tay, C. C., Liu, Z., Wang, W., & Hu, B. (2025). Efficient adsorption and reduction of Au (III) to gold particles using cost - effective chitosan functionalized cellulose nanofiber. *Carbon Research*, *4*(12), 1–11. https://doi.org/10.1007/s44246-024-00176-3

Wang, J.; Chen, C. (2009). Biosorbents for Heavy Metals Removal and Their Future. *Biotechnol. Adv.* 2009, 27, 195–226

Wang, Y., You, L., Lyu, H., Liu, Y., & He, L. (2022). Role of biochar – mineral composite amendment on the immobilization of heavy metals for Brassica chinensis from naturally contaminated soil. *Environmental Technology & Innovation*, *28*, 1–14. https://doi.org/10.1016/j.eti.2022.102622

Yahya, M. D., Abubakar, H., Obayomi, K. S., Iyaka, Y. A., & Suleiman, B. (2020). Simultaneous and continuous biosorption of Cr and Cu (II) ions from industrial tannery effluent using almond shell in a fixed bed column. *Results in Engineering*, *6*(March), 100113. https://doi.org/10.1016/j.rineng.2020.100113

Yang, Z., Wang, J., Zhao, N., Pang, R., Zhao, C., Deng, Y., & Yang, D. (2024). A novel biochar - based 3D composite for ultrafast and selective Cr (VI) removal in electroplating wastewater. *Biochar*, *6*(46), 1–17. https://doi.org/10.1007/s42773-024-00338-x

Yuan, J., Wang, C., Tang, Z., Chu, T., Zheng, C., Han, Q., Chen, H., & Tan, Y. (2024). Biochar derived from traditional Chinese medicine residues : An efficient adsorbent for heavy metal Pb (II). *Arabian Journal of Chemistry*, *17*(3), 105606. https://doi.org/10.1016/j.arabjc.2024.105606

Zhang, N., Reguyal, F., Praneeth, S., & Sarmah, A. K. (2023). A novel green synthesized magnetic biochar from white tea residue for the removal of Pb (II) and Cd (II) from aqueous solution : Regeneration andsorption mechanism. *Environmental Pollution*, *330*(May), 121806. https://doi.org/10.1016/j.envpol.2023.121806

Zhu, S., Qu, T., Kashif, M., & Jianying, I. (2020). Simultaneous removal of Cd (II) and As (III) from co - contaminated aqueous solution by α - FeOOH modified biochar. *Biochar*, 1–12. https://doi.org/10.1007/s42773-020-00040-8